20. Miles, G. D., L. Shedlovsky, and J. Ross, *J. Phys. Chem.*, 49, 93 (1945).
21. Mysels, K. J., K. Shinoda, and S. Frankel, "Soap Films, Studies of their Thinning and a Bibliography," Pergamon Press, New York (1959).
22. Osipow, L. I., "Surface Chemistry, Theory and Industrial Applications," ACS Monograph Series 153, Reinhold, New York (1962).
23. Ross, S., *J. Phys. Chem.*, 47, 266 (1943).
24. Rubin, E., and E. L. Gaden, Jr., "New Chemical Engineering Separation Techniques," Chap. 5, H. M. Schoen, ed., Interscience, New York (1962).
25. Schnepf, R. W., and E. L. Gaden, Jr., *J. Biochem. Microbiol. Tech. Eng.*, 1, 1 (1959).
26. ———, E. Y. Mirocznik, and E. Schonfeld, *Chem. Eng. Progr.*, 55, No. 5, p. 42 (1959).

Manuscript received March 23, 1964; revision received August 14, 1964; paper accepted September 9, 1964.

Part II. Experimental Verification and Observations

Experimental results obtained over a wide range of variables from three different foam fractionation columns support the theory developed in Part I.

In Part I a theory was developed for interstitial flow in foam which could be applied to foam fractionation. This paper presents the results of experimental tests of this theory.

EXPERIMENTAL

A foam fractionation column of 4.1-cm. I.D. was constructed of glass as shown in Figure 1. Thoroughly humidified nitrogen was bubbled up through the liquid pool at the bottom, forming foam which rose up the column and passed out through the horiontal line of 0.8-cm. I.D. at the top. The liquid level of the pool at the bottom of the column was maintained approximately 80 cm. below the overhead foam line. The feed point and pressure probe were adjustable up and down the column. Operation was at 25° ± 1°C. in a temperature-controlled room. Further details of experiments and results have been placed on file (*6*).

A bubbler with a single orifice was employed in order to obtain a uniform bubble size for a given run. The frequency at which bubbles were formed was measured with a stroboscopic light. The bubble diameter was then calculated by $d_{30} = \sqrt[3]{6G/\pi N}$. The feed was a 5×10^{-4} molar aqueous solution of the surfactant Triton X-100, which can be considered to have the formula $C_8H_{17}—\phi—(OCH_2CH_2)_{9.7}—OH$.

After a foam with bubbles of uniform size and known diameter had been formed, the gas flow to the bubbler was usually stopped. The liquid feed rate through the foam was continued for a while to achieve steady state conditions and to allow the flow rate to be checked. Then the feed line was closed and the bottom exit was blocked so that the volume of interstitial liquid in the foam could be measured when the foam collapsed. During these latter operations, the faces of the foam bubbles were observed in order to obtain a measure of their thickness by their progressive color changes with a technique (*1*, *7*) based on the diffraction of incident light.

Two runs were made at continuous gas flow conditions. These required a much longer time to reach steady state and still longer to collect enough overhead foam for a measurement of collapsed volume. Furthermore, it was difficult to maintain the relatively dry foam in the necking section at the top of the column. The strain of the tenfold reduction in cross section would often suddenly collapse all the foam in the entire top section of the column, thus invalidating the run. Accordingly, most of the runs were not of this type involving continuous gas flow, since much of the information that could be obtained from this column could be gained just as well and more quickly by simply letting liquid flow down through stationary foam, that is with $v_{f,\,so} = 0$.

Surface tension was measured with a ring tensiometer yielding values close to those obtained by others (*2*, *4*). Viscosity was measured with an Ostwald viscosimeter, yielding values close to those of pure water. Γ determined from surface tension via Gibbs' equation generally compared favorably with that determined from Equations* (2) and (3) from experiments with the foam column. Both methods yielded Γ of about 2.8×10^{-10} g. moles/sq.cm., except for very dry foams in which a micelle double film (*5*) may have formed. Solute concentrations were measured by ultraviolet spectrophotometry.

RESULTS

For each run, the experimental values for V_L/V_G, t, and $d_{32} = d_{31} = d_{30}$ were substituted in Equation (8) to give A_{PB}. This was for the section of column from the feed point down to the surface of the liquid pool. Substitution in Equation (6) gave r_o. T followed from Equation (17).

Measurements with the pressure probe showed that the entire weight of foam was transmitted as hydrostatic head. Observation of face colors showed no variation of t with height, which implies $dr_o/dz = 0$ and also a uniform foam density. This uniformity in $\mathfrak{D}$ accords with the prediction

* All equation numbers refer to Part I.

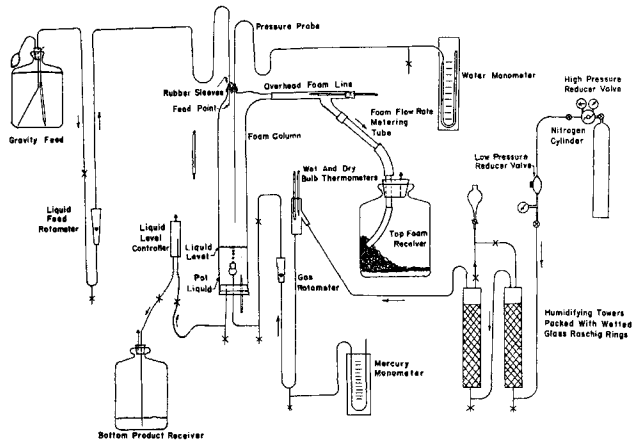

Fig. 1. Apparatus.

of theory in Part I.

Substitution in Equation (18) gave g_{eff}. Then $h_{eff} = \rho g_{eff}/\mu$ where ρ and μ were taken as those for pure water. Velocity $v_{f,so}$ was calculated from Equation (31). As pointed out above, it was zero for most runs. P was evaluated from Equation (7). In view of steady state operation, $W = q_{\text{net down,so}} = -q_{\text{net up,so}}$. Then μ_s was evaluated by simultaneous trial and error solution with Equations (14) (with $v_{z,\max,BO}$ replacing $v_{z,\max}$), (16), (22), and (30), and Figures 3 and 8, with $v_{b,MO} = 0$. Normal exit criteria were not involved here. For all the runs, the values of μ_s thus obtained ranged from 0.24×10^{-4} to 2.24×10^{-4} dyne sec./cm., with a standard deviation of 0.63×10^{-4} dyne sec./cm. The mean value of μ_s was 1.24×10^{-4} dyne sec./cm., with a 95% confidence interval of $\pm 0.40 \times 10^{-4}$ dyne sec./cm. by statistical t test.

At the conclusion of a run, while the foam in the column was allowed to drain preparatory to measurement of V_L/V_G, close inspection of bubbles through a magnifying glass revealed bits of black film forming at the bottom of a face and rising upward in the face. These bits appeared as little circles, each trailed by a thin wavey black tail as illustrated in Figure 2. These circles are local areas of extremely small film thickness and appear black by virtue of diffractive cancellation of light. Being thinner than the surrounding film they float up in the face under the influence of gravity.

A method has been proposed (7) whereby these black circles may be used in an independent manner to determine an approximate value for μ_s. Accordingly, for each of sixteen observations, an estimate was made of the film thickness, the inclination of the face, the diameter of the black circle, and the distance the circle moved within the face in a timed interval. These rough measurements were then substituted in the equation given below, which is essentially the surface analogue of Lamb's classical solution

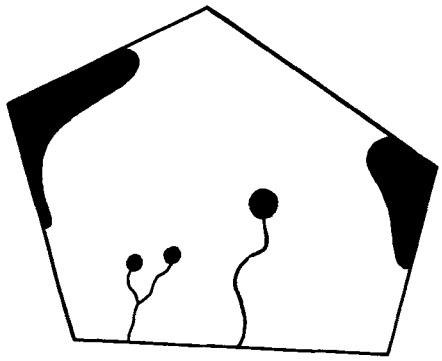

Fig. 2. Typical pattern of black in white film, showing the rising black circles.

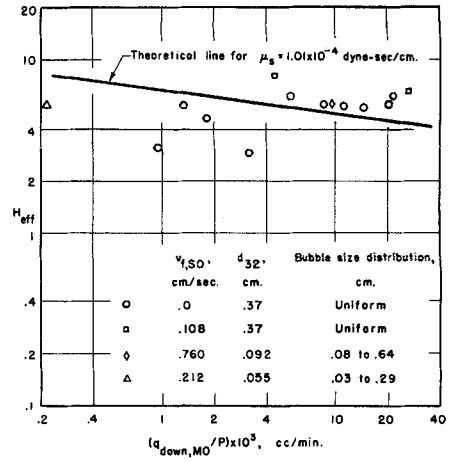

Fig. 3. Experimental results for flow through foam.

for a buoyant, infinitely long, horizontal cylinder rising at terminal velocity in a homogeneous viscous fluid:

$$\mu_s = \frac{-r_c^2 \rho g (t - t_b)\cos\varphi}{8u}\left[0.0772 + \ln\frac{u r_c \rho t}{8\mu_s}\right] - \frac{\mu t}{2}$$

The last term was negligible. Solving by trial yielded values of μ_s ranging from 0.38×10^{-4} to 1.55×10^{-4} dyne sec./cm. with a standard deviation of 0.47×10^{-4} dyne sec./cm. The mean value of μ_s was 1.01×10^{-4} dyne sec./cm., with a 95% confidence interval of $\pm 0.25 \times 10^{-4}$ dyne sec./cm.

When one considers the various experimental uncertainties, μ_s of 1.01×10^{-4} dyne sec./cm. determined from the black circles agrees fairly well with μ_s of 1.24×10^{-4} dyne sec./cm. determined from interstitial flow through foam. This supports the theory developed in Part I. It should be added that altering the theoretical model by assuming $v_{b,MO} \neq 0$ yielded no better agreement.

Figure 3 shows experimental results plotted as H_{eff} vs. $q_{\text{down,MO}}/P$, which is a proportional measure of the flow rate through a Plateau border. For stationary foam, $v_{f,so} = 0$, and so $q_{\text{down,MO}} = q_{\text{net down,so}} = W$. For moving foam, $q_{\text{down,MO}} = W + PA_{PB}v_{f,so}$. Also shown are the results for two additional runs with a multiorificed bubbler that produced a very nonuniform distribution of bubble sizes. For these two runs the distribution was determined by count and measurement of individual bubbles in the narrow part of the neck at the top of the column. This was the original purpose of constructing the narrow takeoff.

For comparison, Figure 3 also shows a curve for H_{eff} vs. $q_{\text{down,MO}}/P$ determined from the theory of Part I by use of the value of μ_s derived by the independent black circle method. The theoretical curve is seen to pass through the general region of the data. In view of the range of variables and the experimental uncertainties, this is deemed to be good agreement.

ADDITIONAL COMPARISONS

Further confirmation for the theory was obtained from the experimental values for the overhead flow D in the runs with $v_{f,so} \neq 0$. This was bolstered with additional runs made very early in the investigation with a nonuniform bubbler in another column designed to accommodate removable plates. (These plates proved to be of no particular advantage.)

Runs for which the feed point was above the exit plane were discarded. Also discarded were runs in which large

wall-to-wall slugs of gas were present, indicating severe breakage of foam. Finally, only runs for which the bubble size distribution was measured along the outlet tube atop the column were used. Measurement of bubble size at the side of a column can sometimes be misleading, since the larger bubbles tend toward the center line and thus are hidden from view by the smaller bubbles at the wall. Furthermore, as pointed out in Part I, taking the bubble sizes at the top minimizes the effect of coalescence on the theory.

A total of eight runs met these criteria. These covered a fairly wide range of experimental variables, namely D from 0.062 to 0.305 cc./sec., $v_{f,so}$ from 0.22 to 0.78 cm./sec., and d_{31} from 0.05 to 0.11 cm. For each run, experimental D was compared with theoretical D from Equation (32) based on the independently determined value of $\mu_s = 1.01 \times 10^{-4}$ dyne sec./cm. Over the eight runs, the ratio of theoretical D to experimental D ranged from 0.86 to 1.95, with a standard deviation of 0.36. The mean ratio was 1.38 ± 0.30 at the 95% confidence level. This is considered reasonably good agreement. However, the modest positive difference over unity is statistically significant. It could be due to the effect of the sharp reduction in cross section experienced by the foam as it enters the outlet tube. It could also be indicative of some experimental bias in determining the bubble size distribution from the nonuniform bubbler employed for these runs. Error at the small diameter end of the distribution curve is especially critical.

Profiting from experience with the columns described above, a different but related investigation was begun. In this new study (3), a foam column was constructed with an overhead takeoff which was not necked. Bubble size distributions were determined visually or photographically at the surface of the liquid pool. Then, as described in Part I, these were corrected for coalescence within the column up to the exit by means of electrical conductivity measurements of foam density.

Some preliminary data from this new study are available. Column diameter is 4.6 cm., which is slightly larger than heretofore. Calibration runs with feed entering near the top showed a uniform foam density, which conforms with the theory. Five usable runs are available with feed entering the liquid pool. D ranged from 0.0014 to 0.0306 cc./sec., $v_{f,so}$ from 0.082 to 0.195 cc./sec., and d_{31} from 0.11 to 0.24 cm. Again utilizing the independent μ_s of 1.01

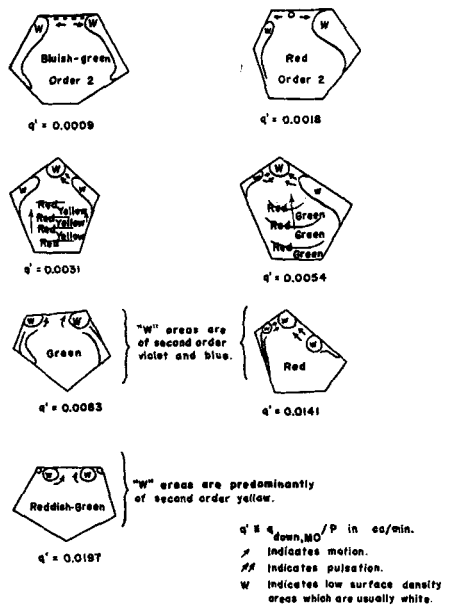

Fig. 4. Typical bubble face patterns in foam.

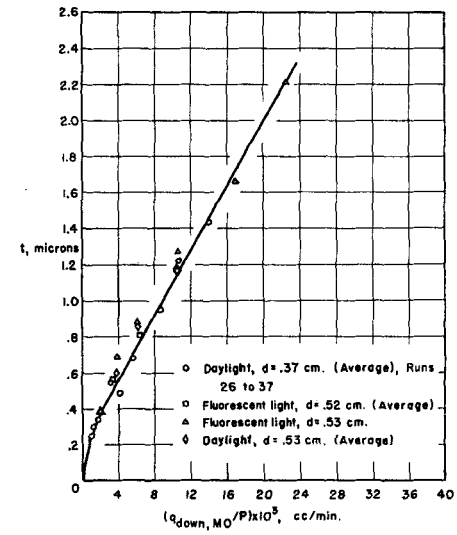

Fig. 5. The effect of interstitial liquid flow on film thickness.

dyne sec./cm., the mean ratio of theoretical D to experimental D ranged from 1.01 to 1.56, with a standard deviation of 0.25. The mean ratio was 1.22 ± 0.31 at the 95% confidence level. In view of the wide range of variables and the difficulty in measuring bubble sizes, this is deemed to be good agreement with theory.*

When one considers the wide range of variables encompassed by the new study and the present study taken together, the experimental results appear to confirm the theory.

BUBBLE FACES

Careful observations were made of bubble faces at steady state conditions in the section of the column between the liquid pool and the feed point. These showed differing colors from face to face, indicating thicknesses differing by as much as 0.3 micron from the average for the particular run. However, as mentioned earlier, no trend of t with height could be discerned. These differences in t among the faces are attributed to differences in orientation and other local factors.

At steady state, the color and hence the local thickness of any one face was largely uniform over the face. However at the top of the face some low surface density regions were visible which were often distorted down the edges of the face by the drag of downward flow in the Plateau borders. In some cases local pulsation was observed. Small swirls were sometime visible at the edges near the intersection of Plateau borders. Alternating lighter and darker ripples of the same color, or sometimes ripples of two alternate colors, were observed to form at the lowest Plateau border of the face and rise up in the face. This suggests that the face may be continuously generated at its bottom and captured at its top by the flow through the Plateau borders.**

All in all, the local facial flow patterns are quite complex. Figure 4 shows some representative observations for steady state conditions. The situation at unsteady state, which is not shown, is even more complex. Upon draining, changing bands of color would appear in a single face which would ultimately turn white with the aforementioned little black circles in evidence.

* As of this writing, more refined data being developed from this new study are yielding even better agreement with theory.

** It is worth mentioning that trial hypotheses of appreciable inequality between $v_{b,MO}$ and zero yielded calculated local stresses which were inconsistent with any reasonable value of μ_s when combined with detailed observations of the faces, especially the small facial distances available to dissipate the stress. However, such inconsistency was not the case with the original hypothesis of $v_{b,MO} = 0$ which is thus supported.

The average film thickness increased with the average flow rate through a Plateau border. This is shown in Figure 5, for which C_L was about 5×10^{-7} g.-moles/cc. The dimensionless thickness T increased approximately linearly from 1.5×10^{-3} to 6×10^{-3} over the same range of experimental $q_{down,MO}/P$.

SUMMARY OF CONCLUSIONS

Observations and flow measurements at steady state were taken in a specially constructed foam column employing stationary foams and moving foams. When combined with surface viscosity measured by an independent method, the experimental results were in substantial agreement with those predicted by the theory developed in Part I. Additional confirmation of the theory was obtained with experimental results from two other columns.

ACKNOWLEDGMENT

The work in Parts I and II was supported directly by U.S. Public Health Research Grant WP-161. Indirect support was derived from the National Science Foundation through grant G-19281 at the University of Cincinnati Computer Center and through a Cooperative Fellowship.

NOTATION

dA = differential area situated in A_{PB}, sq.cm.
dA^+ = dA/A_{PB}
A^+ = dimensionless A_{PB}; that is, unity
a = PB dimension as shown in Figure 2c, cm.
A_{col} = horizontal cross-sectional area of a foam column, sq.cm.
A_h = that part of the horizontal cross-sectional area of a column which cuts through the PBs, sq.cm.
A_{PB} = perpendicular cross-sectional area of a PB, sq.cm.
C = concentration of the surfactant per unit volume of solution, g.-moles/cc.
D = volumetric flow rate of the collapsed overhead foam; that is, of just the liquid content, cc./sec.
D' = volumetric flow rate of the collapsed net overhead product withdrawn when reflux is employed, cc./sec.
$\mathcal{D}$ = volumetric foam density
d_{ek} = average bubble diameter, cm.
d_i = particular bubble diameter, cm.
d_{30} = bubble diameter averaged by volume and number of bubbles, cm.
d_{31} = bubble diameter averaged by volume and diameter, cm.
d_{32} = bubble diameter averaged by volume and area, cm.
E = length of PB, cm.
e = integer
F = volumetric feed rate, cc./sec.
G = volumetric flow rate of gas, cc./sec.
g = gravitational acceleration, cm./sec.^{2}
g_{eff} = effective gravitational acceleration, cm./sec.^{2}
H_{eff} = dimensionless hydrodynamic driving force, $h_{eff}A_{PB}/v_{z,max,BO}$
h_{eff} = $\rho g_{eff}/\mu$, cm.$^{-1}$ sec.$^{-1}$
i = index
k = integer
M = dimensionless viscosity ratio, $\mu r_o/\mu_s$
N = number of bubbles formed per unit time, sec.$^{-1}$
n_i = number of bubbles with diameter d_i
P = packing factor, the total length of PBs within a unit height of foam column
p_{in} = pressure inside the PB, dynes/sq. cm.
p_{out} = pressure outside the PB, dynes/sq. cm.
Q = dimensionless volumetric flow rate, $q/(PA_{PB}v_{z,max,BO})$
q = volumetric flow rate, cc./sec. or cc./min.
q' = $q_{down,MO}/P$, cc./min.
R = reflux ratio
r = radial coordinate, cm.
r_c = radius of a black circle, cm.
r_o = radius of curvature of PB-gas interface, cm.
T = dimensionless cross sectional aspect ratio for a PB, t/r_o
t = film (face) thickness, cm. or microns
t_b = film thickness of a black circle, cm. or microns
u = velocity of a black circle moving within a face, cm./sec.
V_{liq} = volume of liquid in all the PBs confined in the incremental height H, cc.
V = dimensionless velocity, $v/v_{z,max,BO}$
v = velocity, cm./sec.
V_G = volume of gas in a $(V_L + V_G)$ volume of foam, cc.
V_L = volume of liquid in a $(V_L + V_G)$ volume of foam, cc.
W = volumetric bottom product rate, cc./sec.
z = axial coordinate along the PB axis which may be particularized as being vertically downward, cm.

Greek Letters

Γ = surface excess, g.-mole/sq.cm.
γ = surface tension, dynes/cm.
ϵ = void (gas) fraction in the foam
θ = angle which the PB makes with the horizontal
μ = viscosity, dyne sec./sq.cm.
μ_s = surface viscosity, dyne sec./cm.
ρ = liquid density, g./cc.
τ = time, sec.
φ = angle of inclination between the bubble face and the vertical

Subscripts

b = in an axial (z) direction at the border between the PB and the bubble film (such as at point A of Figure 2)
BO = with respect to an observer located at the border between the PB and the bubble film (such as at point A of Figure 2)
D = collapsed overhead foam
down = downward
F = feed
f = of the foam, taken in a vertically upward direction when applied to the foam velocity
L = interstitial liquid free of Γ in the overhead foam
max = maximum, that is at point 0 of Figure 2, which in some contexts is particularized for a vertical PB
MO = with respect to an observer moving with the same vertical velocity as the aggregate of foam bubbles
net = net
r = in a radial direction
R = reflux
SO = with respect to a stationary observer
up = upward
W = bottom liquid product
z = in an axial direction which may be particularized as being vertically downward
θ = in an angular direction
1 = at some level in the column
2 = at another level in the same continuous section of the column

Superscript

o = taken at $V_{f,SO} = 0$ and $V_{b,MO} = 0$

LITERATURE CITED

1. Bikerman, J. J., "Foams: Theory and Industrial Applications," Reinhold, New York (1953).
2. Crook, E. H., D. B. Fordyce, and G. F. Trebbi, *J. Phys. Chem.*, 67, 1987 (1963).
3. Fanlo, S., Ph.D. dissertation, University of Cincinnati, Cincinnati, Ohio, in preparation.
4. Greenwald, H. L., E. B. Kice, M. Kenly, and J. Kelly, *Anal. Chem.*, 33, 465 (1961).
5. Lauwers, A., P. Joos, and R. Ruyssen, "Third International Congress on Detergency, Vol. 3, Sec. C, p. 195, Cologne (1960).
6. Leonard, R. A., Ph.D. dissertation, University of Cincinnati, Cincinnati, Ohio (June, 1964).
7. Mysels, K. J., K. Shinoda, and S. Frankel, "Soap Films, Studies of their Thinning and a Bibliography," Pergamon Press, New York (1959).

Manuscript received March 23, 1964; revision received August 14, 1964; paper accepted September 9, 1964.

Turbulence Characteristics of Liquids in Pipe Flow

GODFREY Q. MARTIN
University of Idaho, Moscow, Idaho
LENNART N. JOHANSON
University of Washington, Seattle, Washington

The turbulence characteristics of a fluid stream in a given duct geometry are of interest in a wide variety of applications. For example, the dispersion of mass and the transfer of heat by turbulent diffusion, problems of particular importance to chemical engineers, are greatly influenced by these turbulence characteristics. Typical parameters used to describe turbulence are the relative intensity and the integral scales of turbulence. These parameters may be obtained from either Lagrangian (observer moves with the fluid) or Eulerian (observer is stationary) methods. The mixing properties of a turbulent fluid are closely related to, and may be predicted from, Lagrangian turbulence parameters. Unfortunately there is, at present, no instrumentation available to measure these quantities directly. Eulerian turbulence parameters, however, can be measured directly with hot-wire or hot-film anemometry. A relation between the Eulerian and Lagrangian turbulence parameters would be very useful even it if was empirical.

Most available data on the relative intensity and integral scales of turbulence in pipe flow appear to have been obtained for air systems. It is considerably more difficult, however, to obtain these data for liquids, particularly ordinary tap water or sea water (*1*). The local physical and electrical properties of these liquids may vary with time and location and may differ considerably from the average fluid properties. These variations lead to erratic readings; consequently, great difficulty may be experienced in obtaining accurate, reproducible values of absolute liquid flow rates with hot-film or wire anemometry techniques. Nevertheless, values of the relative intensity of turbulence, correlation coefficients, and integral scales of turbulence were obtained in this investigation which were directly comparable to those in air. It is believed that this agreement was obtained because all the above parameters are relative values and thus self-compensating.

Further, almost no data on Eulerian integral scales of turbulence have been reported in the Reynolds number range below 200,000. A probable reason for this paucity of data is that low frequency (< 5 cycles/sec.) components in the turbulent signal are encountered, and most conventional electronic instrumentation fails in this region.

This investigation reports data on relative intensity and Eulerian scales of turbulence at the center of a pipe through which water was pumped with velocities ranging from 0.5 to 4.0 ft./sec. (N_{Re} = 19,000 to 160,000). The data are compared with those reported with air as the fluid. Results are correlated, insofar as possible, with the Reynolds number of flow and with eddy diffusivities and Lagrangian turbulence parameters reported by other investigators.

THEORY

Einstein (*2*) showed that the mean square displacement of a particle in Brownian movement, after a long interval of time, may be represented by the equation

$$\overline{Y^2} = [2t]\left[0.57\sqrt{\overline{C^2}}\,l\right] \qquad (1)$$

For molecular diffusion $\left[0.57\sqrt{\overline{C^2}}\,l\right]$ may be replaced by a molecular diffusion coefficient D_{mol} to give

$$\overline{Y^2} = [2t]\,[D_{\text{mol}}]$$

Taylor (*3, 4, 5*) showed that if a number of particles having properties similar to the fluid were released in a field of uniform turbulence, the mean value of the displacement of a particle is given by

$$\overline{Y^2} = [2t]\left[\overline{C^2}\int_0^\infty R_L(t')\,dt'\right] \qquad (3)$$

where $R_L(t') = \overline{C_t C_{t+t'}}/\overline{C_t^2}$ is the Lagrangian correlation coefficient between the velocity of a particle at times t and $t + t'$. If one defines a Lagrangian integral time scale of turbulence $T_L = \int_0^\infty R_L(t')dt'$, Equation (3) becomes

$$\overline{Y^2} = [2t]\,[\overline{C^2}\,T_L] \qquad (4)$$

which may be rearranged to give

$$\overline{Y^2} = [2t]\left[\sqrt{\overline{C^2}}\left\{\sqrt{\overline{C^2}}\,T_L\right\}\right] \qquad (5)$$